Extended electron states in lateral quantum dot molecules investigated with photoluminescence

T. v. Lippen, A. Yu. Silov, and R. Nötzel
COBRA Inter-University Research Institute, Eindhoven University of Technology, 5600 MB Eindhoven, The Netherlands
(Received 14 July 2006; revised manuscript received 22 September 2006; published 14 March 2007)

InAs quantum dot molecules (QDMs) formed by molecular-beam epitaxy on GaAs (311)B substrates through self-organized anisotropic strain engineering are studied by excitation-power-density- and temperature-dependent macro- and microphotoluminescence (PL). An unusual asymmetric broadening, together with a continuous shift toward higher energies of the PL peak position, most prominent for the *p*-type modulation-doped QDMs, is observed with increasing excitation power density. The *n*-type modulation-doped QDMs exhibit a square-shaped PL spectrum, resembling that of modulation-doped quantum wells. In temperature-dependent macro-PL, two distinct minima of the full width at half maximum are observed, indicating thermally activated carrier redistribution within the QDMs through two different channels at lower and higher temperatures. The micro-PL spectra of the *p*-type modulation-doped QDMs exhibit discrete sets of sharp peaks on top of broad PL bands. The number and intensity of the sharp peaks increase with excitation power density. With increasing temperature, the number and intensity of the sharp peaks decrease while the intensity of the broad PL bands increases, in agreement with the carrier redistribution at lower temperatures. Only broad PL bands are observed for the *n*-type modulation-doped QDMs with similar behavior. These results are explained by state filling in the presence of extended electron states formed due to lateral electronic coupling of the quantum dots within the QDMs.

DOI: 10.1103/PhysRevB.75.115414 PACS number(s): 78.67.Hc, 73.21.La, 73.22.−f, 78.55.Cr

INTRODUCTION

With the achievement of precise control over the position of quantum structures, interest has moved toward coupling and coherence of these systems to create artificial matter and to obtain new functional units for applications such as quantum communication and computing.[1] In strongly coupled quantum dot (QD) configurations, the wave functions delocalize due to tunneling, leading to extended states described by a coherent superposition of individual QD wave functions. "Artificial molecules" formed by two or more QDs are extremely interesting, since the interdot coupling can be tuned far from the regimes accessible in natural molecules. Coherent coupling, however, requires strong interdot interactions and a high degree of structural ordering, conditions that are difficult to realize.

The technologically easiest way to realize coupled QDs is by vertical stacking along the growth direction, and such structures have been extensively studied.[2–5] In this case, however, the number of stacked QDs is limited by the formation of defects due to strain accumulation and the coupling is limited to one dimension in each QD column. Therefore, for applications, lateral arrangements of QDs are preferred, which allow for coupling in two or even three dimensions when combined with stacking and enable upscaling to very large numbers of functional units in the growth plane and along the growth direction. Lateral QD coupling has been observed in the two limiting cases of a pair of QDs (Ref. 6) and high-density QD layers.[7,8] Here, we demonstrate two-dimensional coupling of the electron states in lateral QD molecules (QDMs) containing, on average, four or eight QDs (Refs. 9 and 10) by excitation-power-density- and temperature-dependent macro- and microphotoluminescence (PL) spectroscopy. Though the average number of QDs has been reduced to one, this intermediate regime, when fully understood, is anticipated to provide the most complex, advanced functionalities, in analogy with the properties of quantum clusters.[11]

The QDMs are formed by self-organized anisotropic strain engineering by molecular-beam epitaxy (MBE) of (In,Ga)As/GaAs superlattice (SL) templates on GaAs (311)B substrates and the ordering of InAs QDs on top due to local strain recognition. Excitation-power-density-dependent macro-PL reveals an unusual asymmetric broadening of the PL spectra, which is stronger for eight QDs per QDM than for four QDs, together with a continuous high-energy shift of the PL peak. In *p*-type modulation-doped QDMs, the asymmetric broadening and high-energy shift are enhanced. The *n*-type modulation-doped QDMs exhibit a square-shaped PL spectrum, resembling that of modulation-doped quantum wells (QWs). Temperature-dependent macro-PL measurements exhibit two distinct minima of the full width at half maximum (FWHM), which are most pronounced for the modulation-doped QDMs, indicating thermally activated carrier redistribution within the QDMs through two independent channels at lower and higher temperatures.

In the micro-PL of the *p*-type modulation-doped QDMs taken at 3.5 K, discrete sets of sharp peaks (FWHM <1 meV) are observed on top of broad (15 meV) PL bands. The number and intensity of the sharp peaks increase with the excitation power density. With increasing sample temperature, the number and intensity of the sharp peaks decrease while the intensity of the broad PL bands increases with a maximum intensity between 80 and 110 K, in accordance with the carrier redistribution at lower temperatures. The *n*-type modulation-doped QDMs exhibit only broad PL bands with similar behavior. These findings are consistently explained by state filling, thermally activated carrier redistribution, and recombination in the presence of extended elec-

tron states due to lateral electronic coupling of the QDs within the QDMs.

EXPERIMENT

The samples were grown by solid-source MBE on GaAs (311)B substrates. After the deposition of a 250-nm-thick GaAs buffer at 580 °C, the samples were cooled down to 520 °C for (In,Ga)As/GaAs SL growth. Each SL period comprised 3.2 nm $In_{0.37}Ga_{0.63}As$ grown at 520 °C, thin capping by 0.7 nm GaAs at 520 °C, annealing for 2 min at 580 °C, and growth of a 5.5 nm GaAs spacer layer at 580 °C. The number of SL periods was 10, and the last GaAs layer was increased to 15 nm. The growth rates of GaAs and $In_{0.37}Ga_{0.63}As$ were 0.073 and 0.116 nm/s. For InAs QD formation on the ten-period SLs, the substrate temperature was decreased to 470 °C. InAs was deposited to a nominal thickness between 0.5 and 0.6 nm at a growth rate of 0.0013 nm/s. The structural properties of the InAs QD layers were characterized by atomic force microscopy (AFM) in air, showing well-ordered and well-separated QDMs containing, on average, four closely spaced QDs.[10] To obtain an average of eight QDs per QDM, the growth temperature of the (In,Ga)As and thin GaAs cap layers in the SL was lowered to 500 °C. The QD density was $\sim 1 \times 10^{10}$ cm^{-2}. For the PL studies, the InAs QDs were capped by 200 nm GaAs. The *n*- and *p*-type modulation-doped samples were obtained by inserting 30 nm of either Si- or Be-doped (1×10^{18} cm^{-3}) GaAs separated by 8 nm undoped GaAs above the QDMs, respectively. The macro-PL measurements were performed by exciting the samples, placed in a He-flow cryostat, with a cw Ti:sapphire laser operating at 800 nm. The excitation power density was varied from 0.01 to 1000 W/cm^2, the latter resulting in a QD occupation by approximately one electron-hole pair, as deduced from time-resolved differential reflection spectroscopy.[12] The PL signal was dispersed by a single monochromator and detected by a cooled (In,Ga)As linear photodiode array. For micro-PL, a low number of QDMs were selected through aluminum masks with 1×1 μm^2 square openings fabricated by electron-beam lithography. The excitation by the Ti:sapphire laser and detection of the PL were performed through a microscope objective. A triple monochromator and the same (In,Ga)As linear photodiode array were used to disperse and detect the PL with high spectral resolution.[13]

RESULTS

Figure 1 shows the evolution of the PL spectra, taken at 5 K, of the QDMs with an average of eight QDs (a) and of four QDs (b) and of the *p*- and *n*-type modulation-doped QDMs with an average of four QDs [(c) and (d)] upon increasing the excitation power density. The PL band at lower energy originates from the QDMs, while that at higher energy stems from the SL template. The corresponding AFM images of the uncapped QDMs are shown in the insets. With increasing excitation power density, an asymmetric broadening and a continuous shift of the PL peak toward higher energies are observed for the QDMs, as well as for the SLs. In general, the asymmetric broadening of the undoped QDMs with averages of four and eight QDs becomes strong above an onset at about $0.1P_0$ ($P_0=1$ kW/cm^2). At the same excitation power density, the accompanying shift of the PL peak towards higher energies increases as well. The asymmetric broadening is larger for the QDMs containing eight QDs. The low-energy side of the PL spectra remains unchanged upon the increase of the excitation power density, with the PL spectra approaching a square shape.

The *p*-type modulation-doped QDMs [Fig. 1(c)] exhibit stronger asymmetric broadening compared to that of the undoped QDMs with pronounced onset already at $0.01P_0$. The shift of the PL peak toward higher energies is larger as well. The *n*-type modulation-doped QDMs [Fig. 1(d)] exhibit a square-shaped PL spectrum from the lowest excitation power density onward. The additional asymmetric broadening and shift of the PL peak toward higher energies are similar to those of the undoped QDMs with comparable onset at $0.1P_0$. The integrated PL intensities versus excitation power density of the different QDM samples exhibit a linear behavior up to P_0, as shown in Fig. 2. Only for higher excitation power densities does the PL intensity begin to saturate. This implies that the QDM states become fully occupied, which is supported by the simultaneous saturation of the asymmetric broadening and high-energy shift of the PL peak.

Figures 3(a)–3(d) show the temperature dependence of the FWHM measured in the macro-PL of the undoped and modulation-doped QDMs. The excitation power density is $0.02P_0$. The FWHM of the QDMs undergoes two minima: the first one between 30 and 70 K and the second one between 140 and 230 K. The minima are accompanied by an enhanced low-energy shift of the PL peak (not shown here). For the undoped QDMs, the minimum at lower temperatures is less pronounced than the minimum at higher temperatures [Figs. 3(a) and 3(b)]. The minimum at lower temperatures is most noticeable for the *p*- and *n*-type modulation-doped QDMs [Figs. 3(c) and 3(d)] and of similar depths as the minimum at higher temperatures.

The macro-PL measurements of the QDMs have revealed unusual effects, i.e., asymmetric broadening together with a shift of the PL peak toward higher energies and two minima in the temperature dependence of the FWHM. Since these effects are the most prominent for the modulation-doped QDMs, we investigate those in detail by micro-PL. In the excitation-power-density-dependent micro-PL spectra of the *p*-type modulation-doped QDMs taken at 3.5 K [Fig. 4(a)], two discrete sets of sharp (<1 meV) peaks superimposed on top of broad (~ 15 meV) PL bands are observed. The number and intensity of the sharp peaks within each set and the intensity of the broad PL bands increase with excitation power density. The *n*-type modulation-doped QDMs, on the other hand, only reveal broad PL bands of similar widths without sharp peaks, whose intensity similarly increases with excitation power density [Fig. 4(b)]. As a function of temperature, the number and intensity of the sharp peaks of the *p*-type modulation-doped QDMs decrease [Fig. 4(c)]. The sharp peaks vanish around 60 K and the intensity of the broad PL bands increases, with a maximum in the temperature range of 80–110 K, before it drops for higher temperatures. For the *n*-type modulation-doped QDMs [Fig. 4(d)], the tempera-

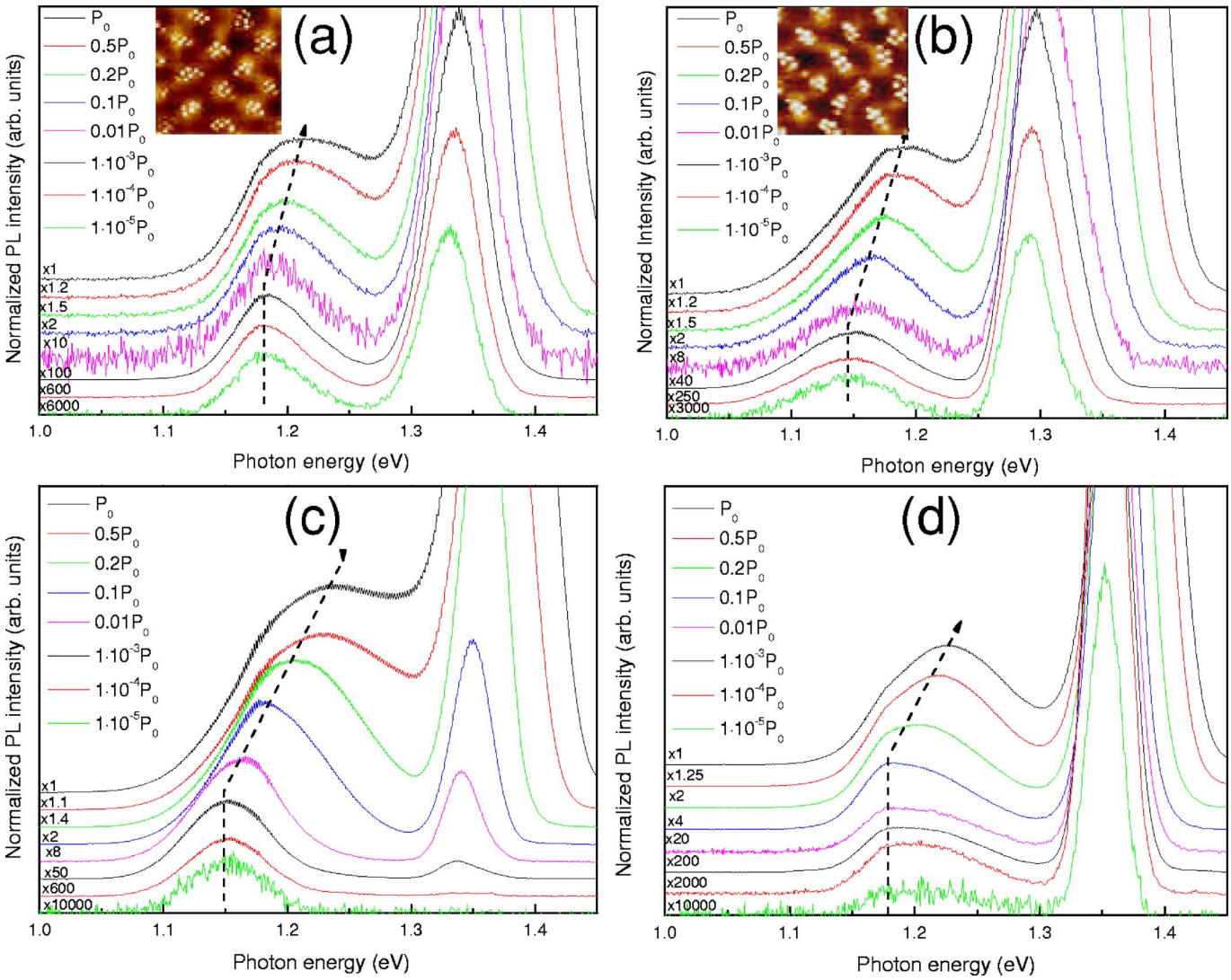

FIG. 1. (Color online) [(a)–(d)] Excitation-power-density-dependent macro-PL spectra, taken at 5 K, of the QDMs with averages of eight (a) and four (b) QDs, and of the *p*-type (c) and *n*-type (d) modulation-doped QDMs with an average of four QDs. $P_0=1$ kW/cm^2. The dotted lines connect the peak intensities as guides for the eyes. The insets (a) and (b) show the AFM images of the QDMs with averages of eight and four QDs.

ture dependence of the intensity of the broad PL bands is similar to that for the *p*-type modulation-doped QDMs. The width of the broad PL bands for both the *n*- and *p*-type modulation-doped QDMs is comparable with a small thermal broadening at elevated temperatures.

DISCUSSION

Macro-PL: Excitation power density dependence

The asymmetric broadening together with the continuous shift of the PL peak toward higher energies are first indications of the formation of extended states in the QDMs due to tunnel coupling. Tunnel coupling of the QD ground states creates extended states with a distinct energy separation determined by the coupling strength. When probing the ensemble of QDMs, this results in an apparent quasi-two-dimensional density of states when the discrete energy states are blurred due to QD size fluctuations. State filling with increase of the excitation power density then accounts for the asymmetric broadening of the PL spectrum, with unchanged low-energy side, which initiates a shift of the PL peak toward higher energies. This is similar to QWs, with the PL spectrum approaching a square shape for high excitation power density. In the excitation power density regime of asymmetric broadening due to state filling, no saturation of the integrated PL intensity occurs. The larger asymmetric broadening for the QDMs with eight QDs than that for the QDMs with four QDs at high excitation power density is explained by the larger number of extended states increasing their total energy spread.

Our experimental data resemble earlier observations of a continuous shift of the absorption spectra when the QD density in layers of randomly positioned QDs was varied.[15] The continuous shift was caused by the presence of extended states in high-density QD clusters without, however, any

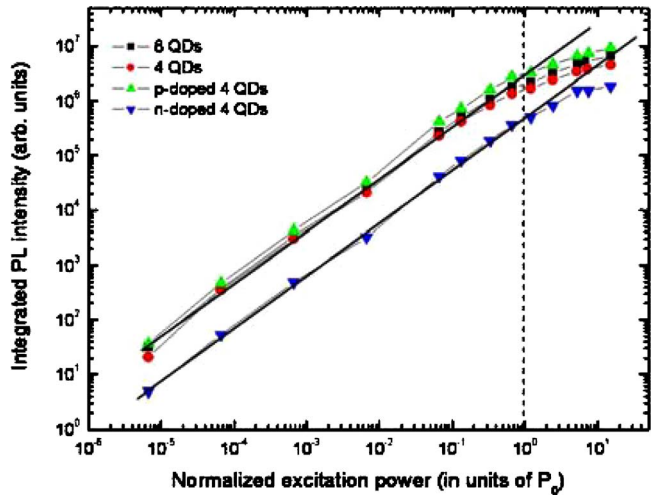

FIG. 2. (Color online) Integrated PL intensity versus excitation power density for the four different QDM samples. The solid and dashed lines are guides for the eyes.

control over the cluster size and position. On the other hand, the behavior of the QDMs is in marked contrast to that of ensembles of isolated QDs, where, with increasing excitation power density, the PL line shape and peak energy of the QD ground-state emission remain unchanged, or even slightly shift to lower energy due to Coulomb interaction, and emission peaks from excited states arise at higher energies due to state filling.[14,15] This is accompanied by a saturation of the QD ground-state emission intensity.

For QDs coupled through phonon assisted tunneling, also a broadening and shift of the PL spectrum toward higher energies would be expected with the increase of the excitation power density when the lower-energy QDs become saturated and higher-energy QDs populated. However, in this case, the shape of the PL spectrum would remain Gaussian for all excitation power densities, reflecting the unperturbed energy distribution of the QD ground states according to the statistic QD size distribution. No fundamental separation of the energy states is present in this case to constitute an apparent two-dimensional density of states of the ensemble of QDMs. However, a contribution to the observed asymmetric broadening and shift of the PL peak toward higher energies

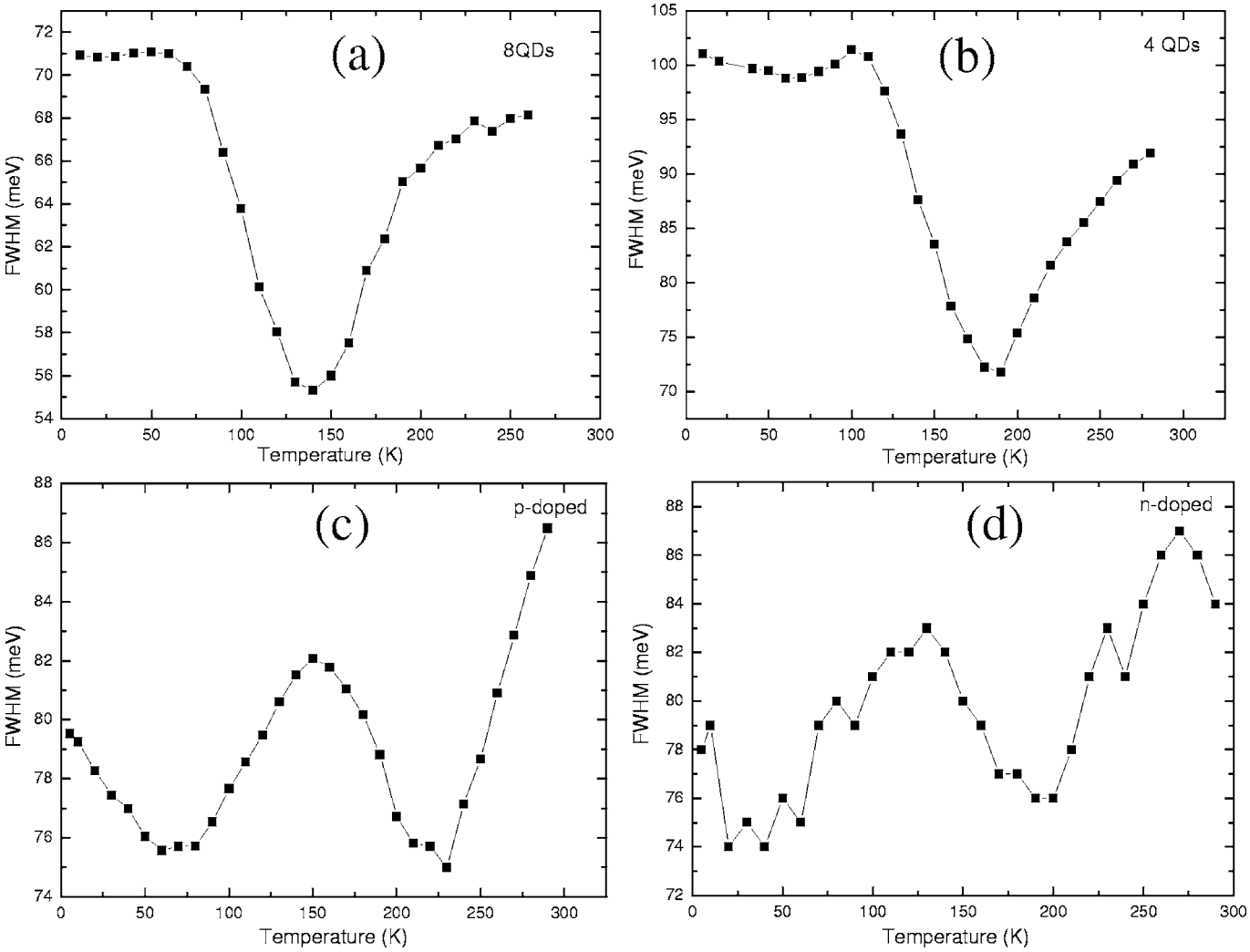

FIG. 3. Temperature dependence of the macro-PL FWHM of the QDMs with averages of eight (a) and four (b) QDs and of the *p*-type (c) and *n*-type (d) modulation-doped QDMs with an average of four QDs. The excitation power density is $0.02P_0$.

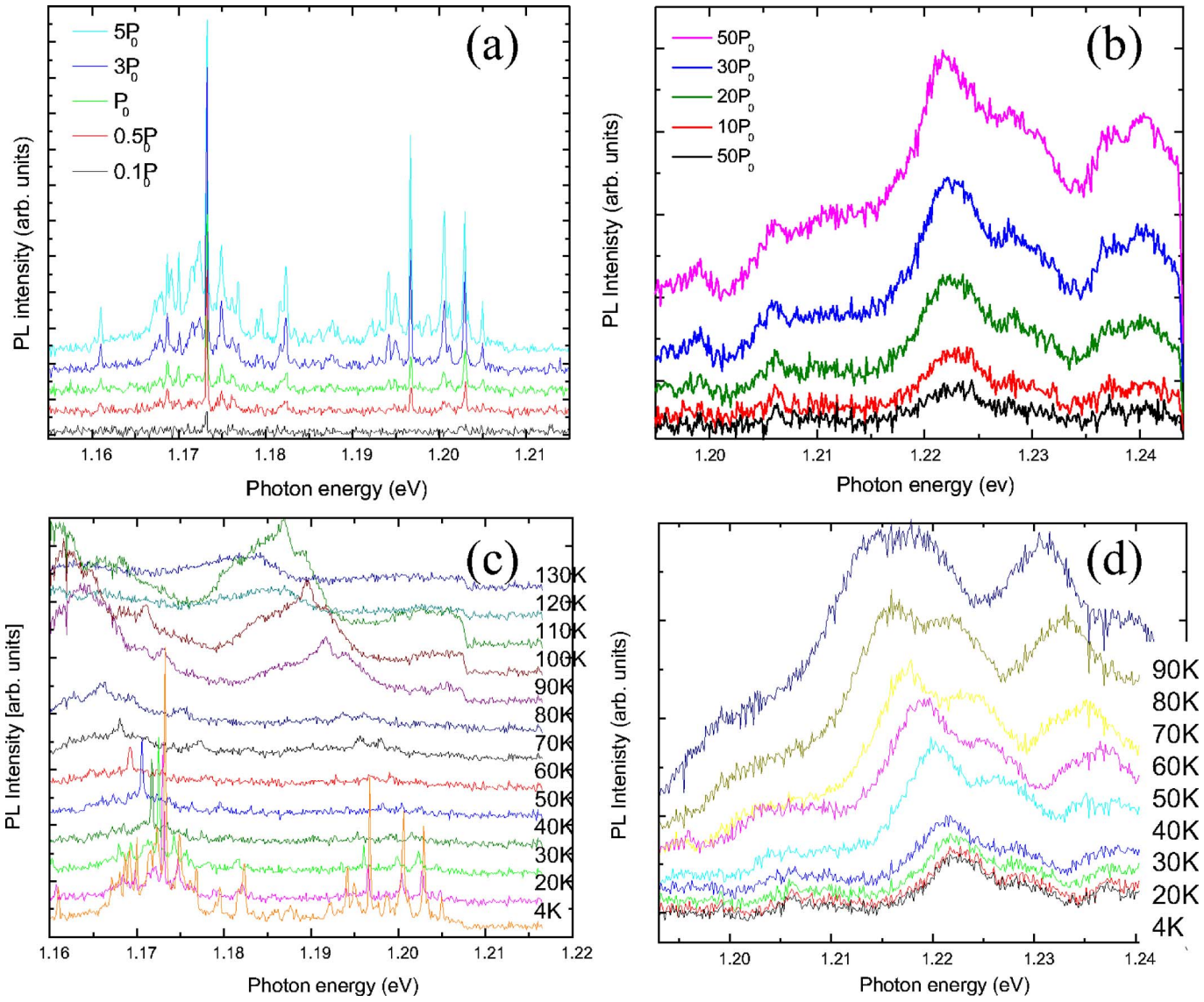

FIG. 4. (Color online) [(a) and (b)] Excitation-power-density-dependent micro-PL spectra, taken at 3.5 K, of the (a) *p*-type and (b) *n*-type modulation-doped QDMs with an average of four QDs. [(c) and (d)] Temperature-dependent micro-PL spectra of the (c) *p*-type and (d) *n*-type modulation-doped QDMs. The excitation power densities are (c) $5P_0$ and (d) $10P_0$ and for (c) the spectral window is determined by the intermediate slits of the monochromator, causing the cutoff at 1.207 eV.

of the QDMs, stemming from the saturation of localized states coupled through phonon assisted tunneling, cannot be excluded. Such localized states or QDs which do not contribute to the extended states form when the unperturbed QD ground-state energies deviate by more than the tunnel coupling splitting due to QD size fluctuations and variations of the QD distances.

The stronger asymmetric broadening and shift of the PL peak toward higher energies of the *p*-type modulation-doped QDMs, with onset already at $0.01P_0$ compared to those of the undoped QDMs with onset at $0.1P_0$, suggests the formation of extended states only for electrons while the holes are localized due to their larger effective mass. *p*-type modulation doping provides a uniform positive background charge, which is not present for the undoped QDMs. This suppresses localization of electrons bound to localized holes, thus favoring extended electron states already for lower excitation power densities before the hole states are filled optically.

The existence of extended electron states is confirmed by the *n*-type modulation-doped QDMs. The square-shaped PL spectrum observed at low excitation power density resembles that of modulation-doped QWs,[16] where all electrons up to the Fermi energy contribute to the emission. From the width of the square-shaped spectrum, a Fermi energy ~50 meV is extracted. This is of the same magnitude as the Fermi energy determined from the doping concentration and from the two-dimensional carrier concentration of a modulation-doped reference (In,Ga)As quantum well of 10–100 meV, keeping in mind the uncertainty of electron transfer efficiency from the doped layer to the QDMs.

The shift of the PL peak toward higher energies might have a contribution from piezoelectric effects[17,18] in the strained QDMs, i.e., the screening of the internal piezoelectric field by photogenerated carriers. The observed magni-

tude of the PL peak shift of about 50 meV is, however, by far larger than the energy shift of 5–10 meV due to piezoelectric effects occurring in isolated QDs on GaAs (311)B.[17] Hence, a significant contribution to the large shift of the PL peak due to piezoelectric effects can only be explained by the presence of extended states. This strongly enhances the influence of the lateral component of the piezoelectric field as the potential change across the QDMs is directly proportional to the extension of the wave function.[18]

Macro-PL: Temperature dependence

The observation of the minima of the FWHM in temperature-dependent macro-PL measurements of QD arrays generally reveals thermally activated redistribution of carriers between QDs of different size and energy. For the QDMs, the unusual observation of the two distinct minima of the FWHM indicates two different carrier redistribution channels at lower and higher energies. The minimum at higher temperature is observed for all kinds of QD arrays and attributed to thermally activated carrier redistribution through the QD wetting layer and barriers.[19] The minimum is due to preferential carrier transfer from smaller (higher energy) to larger (lower energy) QDs with temperature increase, which is followed by equilibration of the carrier distribution in the larger and smaller QDs when the probability of carrier escape becomes comparable. For the QDMs, this translates into thermally activated carrier redistribution through the wetting layer and GaAs barriers between localized states of different energy, which arise due to QD size fluctuations and variations of the QD distances.[20]

The minimum at lower temperature, not observed in ensembles of isolated QDs, cannot be explained by carrier redistribution through the wetting layer and barriers. This minimum indicates a carrier redistribution channel, which is much closer in energy to the localized states, evidencing the presence of extended states which are formed for electrons. The minimum is most noticeable for the *p*-type modulation-doped QDMs, where the formation of extended electron states is favored, in agreement with the larger asymmetric broadening and shift of the PL peak towards higher energies in the excitation power-density-dependent macro-PL measurements.

Micro-PL: Excitation power density and temperature dependences

The presence of extended states in the QDMs manifests itself in the excitation-power-density- and temperature-dependent micro-PL measurements of the modulation-doped QDMs, where the largest effects are observed in macro-PL. The discrete sets of sharp peaks superimposed on broad PL bands for the *p*-type modulation-doped QDMs are attributed to the emission of individual QDMs. The observation of the broad PL bands down to the lowest excitation power density and temperature is a clear signature of the recombination of excitons in quasi-two-dimensional extended states, while the superimposed sharp features originate from the localized states therein.[21] As the localized states in the QDMs arise from QD size fluctuations and variations of the QD distances, their energies can be distributed from below to above the energy range of the extended states. Interestingly, almost all localized states fall in energy within the energy range of the extended states. For the lowest excitation power densities, only a very small number of sharp peaks are observed in each set, smaller than the number of QDs per QDM. With the increase of the excitation power density, additional sharp peaks arise, which are, similar to isolated QDs, attributed to localized biexcitons and charged excitons.

With moderate increase of the temperature, the localized excitons redistribute through the extended states, resulting in the observed gradual reduction of the number of sharp peaks. Further temperature increase then leads to an increase in the intensity of the broad PL bands due to thermally activated occupation of the extended states. The temperature of about 60 K, where the sharp peaks vanish and the intensity of the broad PL bands increases, coincides with the lower temperature minimum of the FWHM in macro-PL, confirming the carrier redistribution through extended states. Moreover, the temperature range of the maximum intensity of the broad PL bands between 90 and 110 K and the successive drop, approaching the higher temperature minimum of the FWHM in macro PL, agrees with redistribution and loss of carriers within the wetting layer and barriers. The absence of sharp peaks for the *n*-type modulation-doped QDMs is attributed to the occupation of the localized states as well as the extended electron states. The localized state emission is buried beneath the stronger emission of the occupied extended electron states, and only the broad PL bands from individual QDMs are observed.

CONCLUSIONS

In conclusion, we have studied excitation-power-density- and temperature-dependent macro- and microphotoluminescence (PL) of ordered lateral quantum dot (QD) molecules (QDMs), indicating the formation of extended electron states. Asymmetric broadening of the macro-PL spectra, which is stronger for eight QDs per QDM than for four QDs, is observed together with a shift of the PL peak position toward higher energies with increasing excitation power density. The asymmetric broadening and high-energy shift of the PL peak are enhanced in *p*-type modulation-doped QDMs. The *n*-type modulation-doped QDMs exhibit a square-shaped PL spectrum, resembling that of modulation-doped QWs. The temperature-dependent macro-PL measurements reveal two distinct minima of the full width at half maximum, implying thermally activated carrier redistribution within the QDMs through two independent channels at lower and higher temperatures. The micro-PL spectra of the *p*-type modulation-doped QDMs exhibit discrete sets of sharp PL peaks on top of the broad PL bands. The number and intensity of the sharp peaks increase with excitation power density. When increasing the temperature, the number and intensity of the sharp peaks decrease while the intensity of the broad PL bands increases, in accordance with the carrier redistribution at lower temperature. Only broad PL bands are observed for the *n*-type modulation-doped QDMs with similar behavior.

These findings are consistently explained by state filling in the presence of extended electron states. They are formed due to lateral electronic coupling of the QDs within the QDMs and appear as a quasi-two-dimensional density of states when probing a large ensemble, resulting in the asymmetric broadening and high-energy shift of the macro-PL spectra as a function of excitation power density. They provide the lower temperature carrier redistribution channel observed in the macro- and micro-PL measurements and account for the broad PL bands in micro-PL.

ACKNOWLEDGMENTS

Part of this research is supported by NanoNed, a technology programme of the Dutch ministry of Economic Affairs via the foundation STW.

[1] D. Bouwmeester, A. Ekert, and A. Zeilinger, *The Physics of Quantum Information* (Springer, Berlin, 2000).
[2] Q. Xie, A. Madhukar, P. Chen, and N. P. Kobayashi, Phys. Rev. Lett. **75**, 2542 (1995).
[3] G. S. Solomon, J. A. Trezza, A. F. Marshall, and J. S. Harris, Jr., Phys. Rev. Lett. **76**, 952 (1996).
[4] J. Tersoff, C. Teichert, and M. G. Lagally, Phys. Rev. Lett. **76**, 1675 (1996).
[5] M. Bayer, P. Hawrylak, K. Hinzer, S. Fafard, M. Korkusinski, Z. R. Wasilewski, O. Stern, and A. Forchel, Science **291**, 451 (2001).
[6] G. J. Beirne, C. Hermannstädter, L. Wang, A. Rastelli, O. G. Schmidt, and P. Michler, Phys. Rev. Lett. **96**, 137401 (2006).
[7] S. Lan, K. Akahane, H.-Z. Song, Y. Okada, M. Kawabe, T. Nishimura, and O. Wada, Phys. Rev. B **61**, 16847 (2000).
[8] S. Lan, K. Akahane, H.-Z. Song, Y. Okada, M. Kawabe, T. Nishimura, and O. Wada, J. Appl. Phys. **88**, 227 (2000).
[9] T. van Lippen, R. Nötzel, G. J. Hamhuis, and J. H. Wolter, Appl. Phys. Lett. **85**, 118 (2004).
[10] T. van Lippen, R. Nötzel, G. J. Hamhuis, and J. H. Wolter, J. Appl. Phys. **97**, 44301 (2005).
[11] T. Maier, M. Jarrell, T. Pruschke, and M. H. Hettler, Rev. Mod. Phys. **77**, 1027 (2005).
[12] E. W. Bogaart, J. E. M. Haverkort, T. J. Eijkemans, T. Mano, R. Nötzel, and J. H. Wolter, J. Appl. Phys. **98**, 073519 (2005).
[13] M. V. Artemyev, A. I. Bibik, L. I. Gurinovich, S. V. Gaponenko, and U. Woggon, Phys. Rev. B **60**, 1504 (1999).
[14] M. J. Steer, D. J. Mowbray, W. R. Tribe, M. S. Skolnick, M. D. Sturge, M. Hopkinson, A. G. Cullis, C. R. Whitehouse, and R. Murray, Phys. Rev. B **54**, 17738 (1996).
[15] R. Heitz, O. Stier, I. Mukhametzhanov, A. Madhukar, and D. Bimberg, Phys. Rev. B **62**, 11017 (2000).
[16] Y. H. Zhang, N. N. Ledentsov, and K. Ploog, Phys. Rev. B **44**, 1399 (1991).
[17] A. Patanè, A. Levin, A. Polimeni, F. Schindler, P. C. Main, L. Eaves, and M. Henini, Appl. Phys. Lett. **77**, 2979 (2000).
[18] R. Nötzel, M. Ramsteiner, Z. Niu, H.-P. Schönherr, L. Däweritz, and K. H. Ploog, Appl. Phys. Lett. **70**, 1578 (1997).
[19] S. Sanguinetti, M. Henini, M. Grassi Alessi, M. Capizzi, P. Frigeri, and S. Franchi, Phys. Rev. B **60**, 8276 (1999).
[20] S. Lan, S. Nishikawa, H. Ishikawa, Q. Wada, K. Akahane, H.-Z. Song, Y. Okada, and M. Kawabe, Jpn. J. Appl. Phys., Part 1 **41**, 2807 (2002).
[21] F. Intonti, V. Emiliani, C. Lienau, T. Elsaesser, R. Nötzel, and K. H. Ploog, Phys. Rev. B **63**, 075313 (2001).